

# Cosmic microwave background constraints on lens spaces

Jean-Philippe Uzan\*

*Institut d'Astrophysique de Paris, GR $\varepsilon$ CO, FRE 2435-CNRS, 98bis boulevard Arago, 75014 Paris, France  
Laboratoire de Physique Théorique, CNRS-UMR 8627,  
Université Paris Sud, Bâtiment 210, F-91405 Orsay cédex, France*

Alain Riazuelo†

*Service de Physique Théorique, CEA/DSM/SPhT, Unité de recherche associée au CNRS,  
CEA/Saclay F-91191 Gif-sur-Yvette cédex, France*

Roland Lehoucq‡

*CEA-Saclay, DSM/DAPNIA/Service d'Astrophysique, F-91191 Gif-sur-Yvette cédex, France*

Jeffrey Weeks§

*15 Farmer St., Canton NY 13617-1120, USA*

(Dated: 22 October 2003)

This article describes the Cosmic Microwave Background anisotropies expected in a closed universe with the topology of a lens space  $L(p, q)$  and with density parameter  $\Omega_0$  close to 1. It provides the first simulated maps for such spaces along with their corresponding power spectra. In spite of our initial expectations that increasing  $p$  (and thus decreasing the size of the fundamental domain) should suppress the quadrupole, we found just the opposite: increasing  $p$  elevates the relative power of the low multipoles, for reasons that have since become clear. For  $\Omega_0 = 1.02$ , an informal “by eye” examination of the simulated power spectra suggests that  $p$  must be less than 15 for consistency with WMAP’s data, while geometric considerations imply that matching circles will exist (potentially revealing the multi-connected topology) only if  $p > 7$ . These bounds become less stringent for values of  $\Omega_0$  closer to 1.

PACS numbers: 98.80.-q, 04.20.-q, 02.040.Pc

## I. INTRODUCTION

High resolution full sky cosmic microwave background (CMB) maps are now available from the Wilkinson Microwave Anisotropy Probe (WMAP) experiment [1], offering an unprecedented opportunity to probe the global structure of our universe (see Refs. [2] for reviews). This article discusses expected CMB anisotropies in spherical spaces, providing simulated CMB maps and their corresponding power spectra produced using the methods of our companion papers [3, 4].

The recent WMAP results interestingly indicate that a closed universe seems to be marginally preferred [1]. In particular, with a prior on the Hubble constant, one gets a density parameter  $\Omega_0 = 1.03 \pm 0.05$ , while further including type Ia supernovae data leads to  $\Omega_0 = 1.02 \pm 0.02$ . Moreover, the WMAP angular correlation function seems to lack signal on scales larger than 60 degrees [1]. This may indicate a possible discreteness and a cutoff in the initial power spectrum, as would be expected from a multiconnected topology. Contrary to the standard lore, we will see that for lens spaces  $L(p, q)$  the topology

leads to an increase of the CMB power on large angular scales. This boost of power is related to the fact that space becomes more and more anisotropic as  $p$  increases. The same effect also appears for (flat) slab and chimney spaces [4, 5] but not in a well-proportioned space as the Poincaré dodecahedral space [6]. In addition, cosmological data indicate that  $|\Omega_0 - 1|$  is small, which has important implications concerning the observability of the topological structure of our universe [7].

It is unlikely that we could detect a compact hyperbolic space if  $\Omega_0 - 1$  is small and negative, because, for a generic observer, the topology scale is comparable to the curvature radius or longer. Only an observer lucky enough to live near a short closed geodesic could detect topology [8].

In flat universes, the topological scale is completely independent of the horizon radius, because Euclidean geometry has no preferred scale and admits similarities. There is no fundamental reason for the topology scale to be less than the horizon radius but still large enough to accommodate the lack of obvious local periodicity. Compact flat universes have nevertheless been studied extensively. In particular, it was shown on the basis of the COBE data that, for a vanishing cosmological constant, no more than 8 copies of the fundamental cell within our horizon are allowed [9]. A non-vanishing cosmological constant relaxes the constraint to 49 copies [10] if  $\Omega_\Lambda = 0.9$  and  $\Omega_m = 0.1$ . A catalog of maps for all flat

---

\*Electronic address: uzan@iap.fr

†Electronic address: riazuelo@iap.fr

‡Electronic address: lehoucq@cea.fr

§Electronic address: weeks@northnet.org

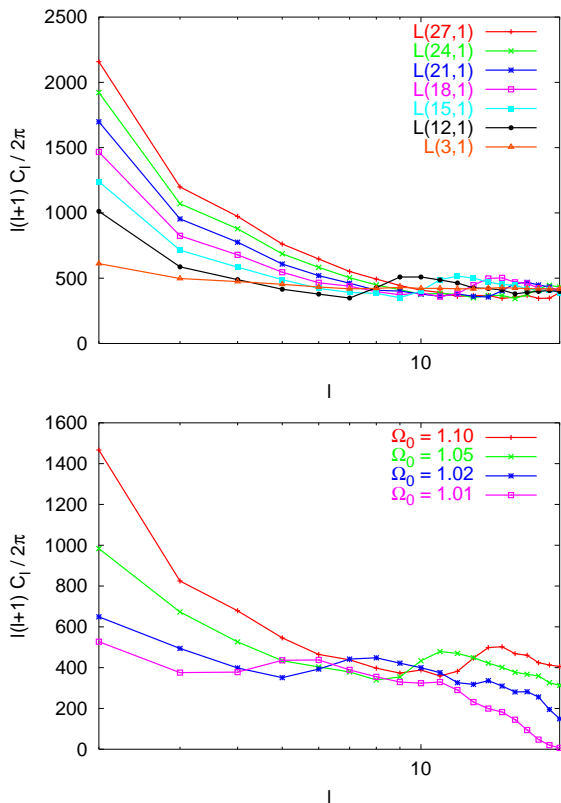


FIG. 1: The angular power spectrum for the lens spaces  $L(p, 1)$  with  $p = 3, 12, 15, 18, 21, 24, 27$  for  $\Omega_0 = 1.1$ . The relative power of the large angular scale increases with  $p$  [top]. Bottom panel shows lens space  $L(18, 1)$  and  $\Omega_0 = 1.01, 1.02, 1.05, 1.1$ . Here, the increase of power on large scales is due to the usual Integrated Sachs-Wolfe effect. (The cutoff at smaller angular scales is unphysical and is simply due to the fact that we used an insufficient number of small wavelength modes.)

spaces (compact, chimney and slab) will soon be available [4].

In spherical spaces the topology scale is tied to the curvature radius, but as the topology gets more complicated, the typical shortest distance between two topological images decreases. So, no matter how flat the universe, all but a finite number of spherical topologies remain detectable.

## II. SPHERICAL MULTICONNECTED SPACES

Three-dimensional spherical spaces were originally classified by Threlfall and Seifert [11] in 1930. The classification was recently revisited in terms of single, double and linked action manifolds by Gausmann *et al.* [12]. Borrowing from Thurston's approach [13], we used the fact that any finite group of unit quaternions determines a fixed point free group  $\Gamma$  of isometries of  $\mathbf{S}^3$ , which then serves as the holonomy group of a multiply connected

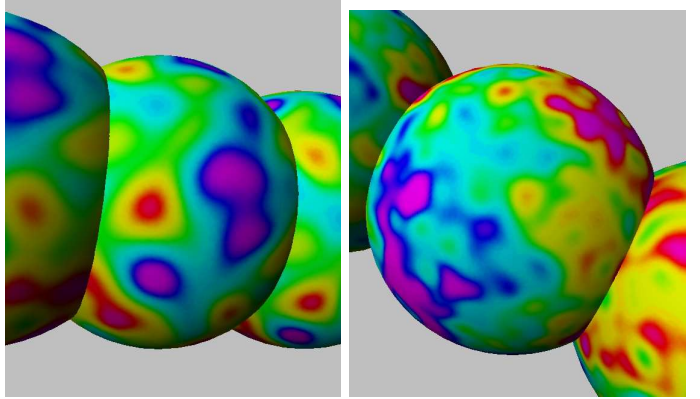


FIG. 2: Simulated maps for the lens space  $L(12, 1)$ . Matching circles are opposite but match with a twist of  $2\pi/p$ . When  $\Omega_0 = 1.02$  [left] there is a single pair of circles; when  $\Omega_0 = 1.1$  [right] there are three pairs; only the smallest pair of circles is shown.

spherical space. The spaces arising in this way are called *single action* spaces and are in one-to-one correspondence with the finite subgroups of  $\mathbf{S}^3$ , thought of as the group of all unit length quaternions. The finite subgroups of  $\mathbf{S}^3$  are the cyclic groups  $Z_n$ , the binary dihedral groups  $D_m^*$ , the binary tetrahedral, octahedral and icosahedral groups, respectively of order  $n, 4m, 24, 48$  and  $120$ . In a *double action* space, two groups of relatively prime order act simultaneously so that  $\Gamma$  is the product of a cyclic group by either a cyclic or a binary polyhedral group. *Linked action* spaces are similar to double action spaces except that the orders of the factors are not relatively prime and only certain elements of one factor are allowed to act simultaneously with a given element of the other factor. In all cases the volume of the space  $\mathbf{S}^3/\Gamma$  is the volume of the 3-sphere  $\mathbf{S}^3$  divided by the order  $|\Gamma|$  of the holonomy group.

*Lens spaces* can be single action, double action, or linked action. A lens space's fundamental domain is constructed by identifying the two faces of a lens shaped solid with a  $2\pi q/p$  rotation, for relatively prime integers  $p$  and  $q$  such that  $0 < q < p$ . The result is the lens space  $L(p, q)$ . Exactly  $p$  copies of the fundamental domain tile the 3-sphere, their faces lying on great 2-spheres filling a hemisphere of each, just as the 2-dimensional surface of an orange may be tiled with  $p$  sections of orange peel, meeting along meridians spaced  $2\pi/p$  apart. Different lens spaces may share the same abstract holonomy group; for example  $L(5, 1)$  and  $L(5, 2)$  both have  $\Gamma \approx Z_5$  even though the group acts differently in each case. Non-cyclic fundamental groups, by contrast, act in a unique way.

Topology breaks the global isotropy and possibly the global homogeneity of the universe, the only exception being projective space (see Ref. [14, 15]). Consequently, the CMB temperature angular correlation function will depend on the two directions of observation, not only on their relative angle, and possibly on the position of the observer as well. This induces correlations between the

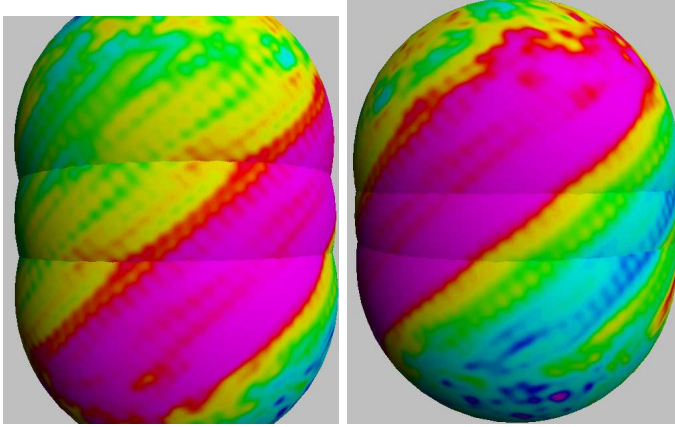


FIG. 3: Same as Fig. 2 but in the extreme case of  $L(100, 1)$  for  $\Omega_0 = 1.1$ . The short period ( $2\pi/100$ ) makes the symmetry along Clifford parallels obvious to the eye.

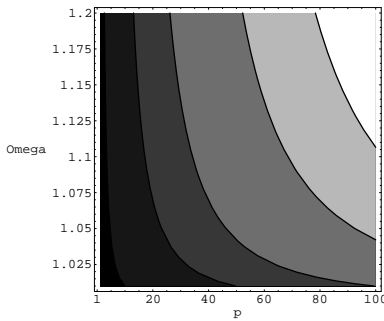


FIG. 4: Number  $N$  of matched circle pairs for a lens space  $L(p, 1)$ , for  $p$  between 1 and 100 and  $\Omega_0$  between 1.01 and 1.2. The contour lines are, from left to right, for  $N = 1, 5, 10, 20, 30$ .

$a_{\ell m}$  of different  $\ell$  and  $m$ . Such correlations are hidden when one considers only the angular correlation function and its coefficients,  $C_\ell$ , in a Legendre polynomial decomposition, because they pick up only the isotropic part and are therefore a poor indicator of the topology. The correlation matrix  $C_{\ell m}^{\ell' m'} \equiv \langle a_{\ell m} a_{\ell' m'}^* \rangle$  encodes all the topological properties of the CMB; see Ref. [3] for details. Conversely, in a simply-connected space it reduces to the usual formula  $C_{\ell m}^{\ell' m'} = C_\ell \delta_{\ell \ell'} \delta_{m m'}$ .

In a companion paper [3], we showed that CMB maps with a topological signal can be confidently simulated for flat and spherical spaces. Topology does not affect local physics and enters only via the boundary conditions of the functions defined on the multi-connected space. Technically, the equations of the cosmological perturbations reduce to a set of coupled differential equations involving the Laplacian operator. They are conveniently solved in Fourier space but this requires the determination of the eigenmodes  $\Upsilon_k^{[\Gamma]}$  with the correct boundary conditions. In  $\mathbb{S}^3$ , the eigenmodes  $\Upsilon_{k \ell m}^{[\mathbb{S}^3]}$  are

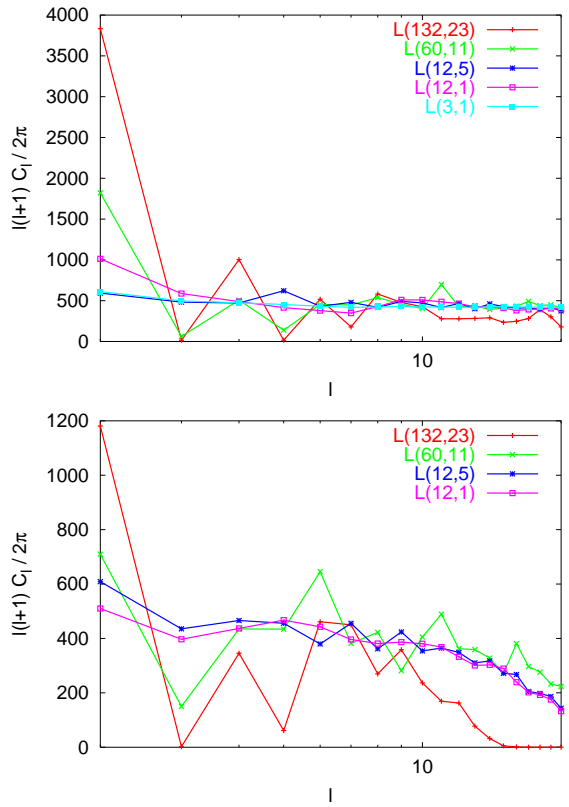


FIG. 5: Influence of the cyclic factors:  $L(12, 5)$  and  $L(12, 1)$  have the same volume but the former typically does not give rise to matching circles;  $L(60, 11)$  and  $L(132, 23)$  both have a cyclic factor  $Z_{12}$  just like  $L(12, 1)$  but have smaller volumes because of an additional factor of  $Z_5$  and  $Z_{11}$ , respectively. Data are shown for  $\Omega_0 = 1.1$  [top] and  $\Omega_0 = 1.02$  [bottom].

labelled by an integer  $\nu$ , related to  $k$  by  $k = (\nu + 1)\sqrt{K}$  where  $K$  is the spatial curvature, and each eigenvalue  $\nu(\nu + 2)K$  has a multiplicity  $(\nu + 1)^2$ . The eigenmodes  $\Upsilon_k^{[\Gamma]}$  can be expressed in terms of the eigenmodes of  $\mathbb{S}^3$  as  $\Upsilon_{k s}^{[\Gamma]} = \sum_{\ell, m} \xi_{k \ell m}^{[\Gamma] s} \Upsilon_{k \ell m}^{[\mathbb{S}^3]}$ , so that all the topological information is encoded in the coefficients  $\xi_{k \ell m}^{[\Gamma] s}$ , where  $s$  indexes the eigenmodes sharing a common value of  $k$ . One finds that the Weyl formula holds for spherical spaces, so a space of order  $|\Gamma|$  has approximately  $N^{[\Gamma]} \sim N^{[\mathbb{S}^3]} / |\Gamma|$  modes [12]. It follows that  $|\Gamma| C_\ell^{[\Gamma]} \rightarrow C_\ell^{[\mathbb{S}^3]}$  when  $\ell$  becomes large [14] (see also Ref. [3] for a numerical check of this behaviour for a torus).

### III. MAPS, POWER SPECTRA AND CONSTRAINTS

For lens and prism spaces the coefficients  $\xi_{k \ell m}^{[\Gamma] s}$  were recently computed analytically using a toroidal coordinate system [16]. CMB codes generally use spherical coordinates but the change of coordinates has been handled [3, 14].

For a homogeneous lens space  $L(p, 1)$ , the parameter  $p$  plays a role analogous (but opposite) to the size  $L$  of a torus in the flat case. The largest spherical 3-manifolds are  $L(1, 1)$  which is the 3-sphere and  $L(2, 1)$  which is projective 3-space. Here we consider the generic case  $p > 2$ . As  $p$  increases, the volume of the space  $L(p, 1)$  decreases. For typical values of  $\nu$  the number of modes diminishes in rough proportion to  $1/p$  according to the Weyl formula. However the  $\nu = 2$  mode has multiplicity 3 for all  $p > 2$ . Thus the  $\nu = 2$  mode has proportionally higher weight in  $L(p, 1)$  than in  $\mathbf{S}^3$ , which explains the excess of power on large angular scales (see Fig. 1). More precisely, after rescaling by the Weyl formula's factor of  $1/p$ , the  $\nu = 2$  mode of  $L(p, 1)$  has an effective multiplicity of  $3/(1/p) = 3p$ , compared to the  $\nu = 2$  mode of  $\mathbf{S}^3$  which has multiplicity 9.

The fact that the smallest nonzero eigenvalue of  $L(p, 1)$  is always  $\nu = 2$  and has constant multiplicity 3 for all  $p > 2$  contrasts sharply to the behavior of the cubic 3-torus of size  $L$ , for which the smallest eigenvalue scales as  $L^{-1}$ . This contrasting behavior can be understood by realizing that as  $p$  increases the space is becoming smaller in only one direction and remains large in perpendicular directions: on large scales we see a 2-dimensional reparation of modes that are perpendicular to the axis of the lens, and the relative weight of large scale as compared to small scales is larger in lower dimensional spaces. An informal examination of Fig. 1 suggests the very conservative upper bound  $p < 15$  when  $\Omega_0 = 1.02$ , for consistency with WMAP's observation of a low quadrupole, keeping in mind that this bound depends on  $\Omega_0$ . This constraint was obtained on the basis of the angular power spectrum only, while a comparison of the full correlation matrix is left for further investigation. This bound on  $p$  was set without any refined statistical analysis mainly because the low  $\ell$  part of the spectrum becomes obviously inconsistent with WMAP data as  $p$  increases. This conservative bound can be used to select the range of a grid for further, more rigorous statistical investigations. Let us also emphasize that our numerical results include all components of the CMB, in particular the Doppler and integrated Sachs-Wolfe contributions, the effects of which were detailed in Ref. [3].

Matching circles [17] occur when the distance  $2\pi/p$  between two closest topological images is less than the diameter of the last scattering surface, as summarized in Table I.

Figure 2 illustrates how the matching circles are diametrically opposite but matched with a twist of  $2\pi/p$ , simply

because Clifford translations twist and translate the same amount. As  $p$  increases, the map becomes more and more anisotropic with obvious twisted structures (Fig. 3). The number of matched circles is given by  $N = p\bar{\chi}_{\text{LSS}}/\pi$  (see Fig. 4).

Recalling that double and linked action spaces combine the action of a cyclic group  $G' = Z_p$  with a more general group  $G$ , let us now consider the effect of the  $G$  factor. As explained in Ref. [7], the nearest repeating images typi-

$\Omega_0 - 1$	0.01	0.02	0.03
$1/\sqrt{K}$ (Gpc)	48.4	34.2	27.9
$\bar{\chi}_{\text{LSS}}$ (rad)	0.316	0.442	0.536
$\text{Vol}(< \bar{\chi}_{\text{LSS}})/\text{Vol}(\mathbf{S}^3)$	0.7%	1.8%	3.1%
detectability	$p \geq 10$	$p \geq 8$	$p \geq 6$

TABLE I: The first three rows give the curvature radius  $1/\sqrt{K}$ , the radius  $\bar{\chi}_{\text{LSS}}$  of the last scattering surface in units of the curvature radius, and the volume of the observable universe as a fraction of the whole universe. The last row gives the constraints on the order  $p$  of the cyclic group so that the topology scale is small enough to be detectable ( $2\pi/p < 2\bar{\chi}_{\text{LSS}}$ ). All numbers are given for  $\Omega_\Lambda = 0.7$ ,  $\Omega_m = 0.32 \pm 0.01$ , and  $h = 0.62$ .

cally depend only on the  $Z_p$  factor, that factor alone may generate matching circles, and circle searching effectively reduces to the case of  $L(p, 1)$ . The  $G$  factor, although typically irrelevant for circle searching, may nevertheless affect the power spectrum. Figure 5 shows power spectra for  $L(3, 1)$  ( $G' = Z_3$ ,  $G$  trivial),  $L(12, 1)$  ( $G' = Z_{12}$ ,  $G$  trivial),  $L(12, 5)$  ( $G' = Z_4$ ,  $G = Z_3$ ),  $L(60, 11)$  ( $G' = Z_{12}$ ,  $G = Z_5$ ), and  $L(132, 23)$  ( $G' = Z_{12}$ ,  $G = Z_{11}$ ). Full understanding of the power spectrum of a general  $L(p, q)$  will require more numerical investigation.

#### IV. CONCLUSION

This article studied the imprint of a lens space topology on the CMB. It provided simulated CMB maps and analyzed potential detectability using the circle matching method. The lens spaces  $L(p, 1)$  generically have a high quadrupole: when  $\Omega_0 = 1.02$ , consistency with WMAP's quadrupole seems to imply  $p < 15$ , while for the same value of  $\Omega_0$  the LSS will intersect itself (and thus produce potentially detectable matching circles) if and only if  $p > 7$ .

---

[1] D.N. Spergel *et al.*, *Astrophys. J. Suppl.* **148** 175 (2003) [[arXiv:astro-ph/0302209](https://arxiv.org/abs/astro-ph/0302209)].  
[2] M. Lachièze-Rey and J.-P. Luminet, *Phys. Rept.* **254** 135, (1995); J. Levin, *Phys. Rept.* **65**, 251 (2002).  
[3] A. Riazuelo *et al.*, *Phys. Rev. D.*, to appear [[arXiv:astro-ph/0212223](https://arxiv.org/abs/astro-ph/0212223)].  
[4] A. Riazuelo *et al.*, in preparation.  
[5] K.T. Inoue and N. Sugiyama, *Phys. Rev. D* **67**, 043003 (2003); M. Douspis *et al.*, to be submitted.  
[6] J.P. Luminet *et al.*, *Nature (London)* **425**, 593 (2003) [[arXiv:astro-ph/0310253](https://arxiv.org/abs/astro-ph/0310253)].  
[7] J. Weeks, R. Lehoucq and J.-P. Uzan, *Class. Quant.*

Grav. **20**, 1529 (2003) [[arXiv:astro-ph/0209389](https://arxiv.org/abs/astro-ph/0209389)].

[8] J. Weeks, Mod. Phys. Lett. A **18**, 2099 (2003) [[arXiv:astro-ph/0212006](https://arxiv.org/abs/astro-ph/0212006)]; G.I. Gomero, M.J. Rebouças, and R. Tavakol, Class. Quant. Grav. **18**, 4461 (2001); G.I. Gomero, M.J. Rebouças, and R. Tavakol, Int. J. Mod. Phys. A **17**, 4261 (2002).

[9] A.A. Starobinsky, JETP Lett. **57**, 622 (1993); D. Stevens, D. Scott, and J. Silk, Phys. Rev. Lett. **71**, 20 (1993).

[10] K.T. Inoue, Class. Quant. Grav. **18**, 1967 (2001).

[11] W. Threlfall and H. Seifert, Math. Annalen **104**, 1 (1930); *ibid.* **107**, 543 (1932).

[12] E. Gausmann *et al.*, Class. Quant. Grav. **18**, 5155 (2001).

[13] W.P. Thurston, *Three-dimensional geometry and topology* (1997) Princeton Mathematical series **35**, S. Levy Ed., (Princeton University Press, Princeton, USA).

[14] R. Lehoucq *et al.*, Class. Quant. Grav. **19**, 4683 (2002).

[15] T. Souradeep, in *Cosmic Horizons*, Festschrift on the sixtieth Birthday of Jayant Narlikar, N. Dadhich and A. Kembhavi Eds. (Kluwer, Dordrecht, 1998).

[16] R. Lehoucq, J.-P. Uzan, and J. Weeks, Kodai Math. Journal **26**, 119 (2003), [[math.SP/0202072](https://arxiv.org/abs/math/0202072)].

[17] N.J. Cornish, D. Spergel, and G. Starkmann, Class. Quant. Grav. **15**, 2657 (1998).